Electronic Supplementary Material (ESI) for New Journal of Chemistry.
This journal is © The Royal Society of Chemistry and the Centre National de la Recherche Scientifique 2021

Supporting Information

Visible-light-responsive lanthanide coordination polymers for highly efficient photocatalytic aerobic oxidation of amines and thiols

Shuyi An,[a] Zhifen Guo,[a] Xin Liu,[a] Yan Che,[a] Hongzhu, Xing [a,]* and Peng Chen[b,]*

[a]Laboratory of Advanced Energy Materials, College of Chemistry, Northeast Normal University, Changchun 130021, P.R. China

[b]Key Laboratory of Functional Inorganic Material Chemistry (MOE), School of Chemistry and Materials Science Heilongjiang University Harbin 150080, P.R. China:

Email: xinghz223@nenu.edu.cn; jehugu@gmail.com

Table of Contents

Materials and methods

All kinds of organic solvents such as DMF, MeCN and dioxane were purchased from InnoChem and used as obtained. Substrates of amines and thiols were purchased from Sigma Aldrich and used as received. Ligand ADBEB was synthesized according to reported procedures.[1,2]

Powder X-ray diffraction (PXRD) patterns were collected at room temperature on a Rigaku SmartLab X-Ray diffractometer operated at 40 kV/30 mA with Cu Kα radiation (λ = 0.15417 nm) and the data collected range of 2θ is from 3° to 40°. The UV-vis DRS spectra of solid samples were recorded on a Cary 7000 spectrophotometer equipped with an integrating sphere. The UV-vis spectrum of ADBEB in DMF was collected on a SHIMADZU UV-2550 spectrophotometer. Thermogravimetric analysis (TGA) were carried out with the Perkin-Elmer TGA-7 thermogravimetric analyzer at a heating rate of 10 ^{o}C min^{-1} from room temperature to 1000 ^{o}C under air atmosphere. Fourier transform infrared (FTIR) spectra were obtained with KBr pellets in the range of 4000–400 cm^{-1} on a Mattson Alpha-Centauri spectrometer. Ln^{3}+ ions were determined with inductively coupled plasma-mass spectrometry (ICP-MS) spectrometer (iCAP-RQ). Scanning electron microscopy (SEM) measurement was taken on a HITACHI SU8000 with an acceleration voltage of 3.0 kV. Photoelectrochemical measurements were measured on CHI 660E electrochemical workstation. Electron paramagnetic resonance (EPR) spectra was recorded on EPR spectrometer (X-band) operated at 9.41 GHz. General parameters are shown as follows: scan range: 100 G; centre field set: 3359.0 G; time constant: 34.18 ms; scan time: 35.00023 s; modulation amplitude: 1.0 G; modulation frequency: 100 kHz; receiver gain: 1.00×10; microwave power: 19.1 mW; measurement temperature: 298 K. Photocatalytic products of imines and disulfides were detected by GC (Shimadzu-Pro-2010) system, where injector port temperature 240 °C, detector temperature 300 °C and column temperature program 6 °C/min from 120 °C to 240 °C sustaining for 10 min. ^{1}H NMR spectra were recorded on 600 MHz spectrometers and were internally referenced to residual deuterated solvent signals ($CDCl_3$, ^{1}H: 7.27 ppm).

Experimental section

Photoelectrochemical measurement

Photoelectrochemical measurements were measured on CHI 660E electrochemical workstation (Chenhua Instrument, Shanghai). The working electrode was made by adding 40 mg CP and 5 mg polyvinylidene fluoride (PVDF) into 1.0 mL ethanol, then the suspension (20 μL) was dropped onto the surface of an ITO plate covering approximately 1 cm^2, then dried at 85 ^{o}C for 2 hours.[3]

Photocurrent measurement was performed in a standard three-electrode system with the photocatalyst-coated ITO as working electrode, Pt plate as counter electrode and Ag/AgCl as reference electrode. 0.2 M Na_2SO_4 solution was used as electrolyte. The photo-responsive signals were measured under 300W Xe lamp where UV and IR filters were used to remove light less than 420 nm and larger than 800 nm. Mott-Schottky plots were also conducted in the same system and the frequency of impedance is set to be 1800, 2000 and 2500Hz, respectively.

Crystal structure determination

Single-crystal X-ray diffraction data of Ln-CPs were collected on a Bruker Smart ApexII CCD diffractometer with graphite-monochromated Mo Kα radiation (λ = 0.71073 Å) at ambient condition. Absorption correction was applied using the multiscan program SADABS.[4] Crystal structure was solved by direct methods and refined by full-matrix least-squares on F^2 with anisotropic displacement using SHELXTL.[5] Lanthanide ions in CPs were easily located, and then non-hydrogen atoms of O, N and C were placed from the subsequent Fourier-difference maps. As shown in Table S1, the details of data collection and refinement are provided. The X-ray crystallographic data of the Ln-CPs reported in this work have been deposited at the Cambridge Crystallographic Data Centre (CCDC) with deposition number of 2045926---2045928. These data can be acquired free of charge from The Cambridge Crystallographic Data Centre via www.ccdc.cam.ac.uk/data_request/cif.

Table S1 Crystal data and refinement of Ln-CPs

Compound	1Tb	1Ho	1Yb
Empirical formula	$C_{36}H_{24}TbNO_7$	$C_{36}H_{24}HoNO_7$	$C_{36}H_{24}YbNO_7$
Formula weight	741.48	747.49	755.60
Crystal system	monoclinic	monoclinic	monoclinic
Space group	$P2_1/c$	$P2_1/c$	$P2_1/c$
a / Å	21.8250(9)	21.6856 (5)	21.5768(5)
b / Å	7.6024(4)	7.62484(19)	7.64833(9)
c / Å	19.0583(11)	19.0898(5)	19.1043(5)
α / °	90	90	90
β / °	109.789(5)	109.625(3)	109.566(3)
γ / °	90	90	90
V / Å^3	2975.4(3)	2973.12(13)	2970.20(14)
Z	4	4	4
F (000)	1472.0	1480.0	1492.0
θ range collected	3.3340 to 28.5080	2.942 to 29.243	3.4750 to 28.7800
Limiting indices	$-26 \leq h \leq 27$ $-7 \leq k \leq 9$ $-24 \leq l \leq 22$	$-27 \leq h \leq 20$ $-6 \leq k \leq 9$ $-23 \leq l \leq 24$	$-27 \leq h \leq 27$ $-9 \leq k \leq 9$ $-16 \leq l \leq 24$
Reflections	14969 /6412	14698 /6420	18972 /6364
Data/restraints/parameters	6412 / 70 / 456	6420 / 76 / 456	6364 /83 / 456
R_{int}	0.0443	0.0396	0.0395
Goodness-of-fit on F^2	1.049	1.075	1.058
R indices (all data)	R_1=0.0499, wR_2=0.0764	R_1=0.0425, wR_2=0.0758	R_1=0.0341, wR_2=0.0593

Table S2 Solvent optimization for photocatalytic benzylamine oxidation[a]

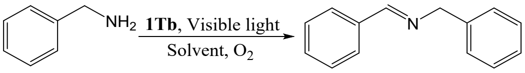

Entry	Solvent	Con. (%)[b]	Sel. (%)[c]
1	DMF	39	99
2	MeCN	3	99
3	CH_3Cl	10	99
4	Dioxane	96	90
5	DMF/Dioxane (1/4)	94	90
6	DMF/Dioxane (1/1)	99	99
7	DMF/Dioxane (4/1)	89	99

[a]Reaction: 7.4 mg of **1Tb**, 1 mL solvent, 0.2 mmol benzylamine, 0.1 mmol biphenyl as an internal standard, O_2 atmosphere, visible light irradiation for 60 min. [b,c]Conversion and selectivity were determined by GC.

Table S3 Visible-light-induced oxidation of benzylamine over CP photocatalysts

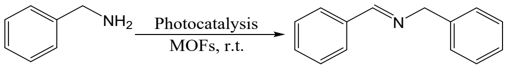

Entry	Photoatalyst	*t* [h]	Conv. [%]	TOF [umol·g^{-1}·h^{-1}]	Refs
1	RPF-30-Er	18	76	72	6
2	RPF-31-Nd	18	60	167	6
3	RPF-31-Sm	18	65	182	6
4	RPF-31-La	18	71	197	6
5	RPF-32-Ho	18	74	208	6
6	UiO-66-NH_2	10	83	333	7
7	NH_2-MIL-125(Ti)	12	73	523	8
8	Cd(dcbpy)	7	99.1	3398	9
9	Zn-bpydc	4	99.7	6231	10
10	NNU-45	2.5	99	9270	11
11	Zn-PDI	4	74	9935	12
12	PCN-222	1	100	10000	13
13	**1Tb**	1	99	13378	this work

Table S4 Solvent optimization for photocatalytic thiol oxidation[a]

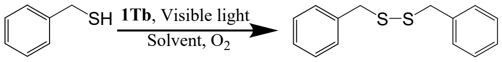

Entry	Solvent	Con. (%) [b]	Sel. (%) [c]
1	DMF	50	99
2	EtOH	15	99
3	MeCN	55	99
4	CH_3Cl	3	99
5	DMF/ MeCN (1/4)	50	99
6	DMF/ MeCN (1/1)	49	99
7	DMF/ MeCN (4/1)	57	99

[a]Reaction: 7.4 mg of **1Tb**, 1 mL solvent, 0.2 mmol benzyl thiol under visible light irradiation for 24 hours, O_2 atmosphere. [b,c]Conversion and selectivity were determined by GC.

Table S5 Quenching experiments for photocatalytic thiol oxidation[a]

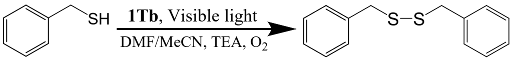

Entry	Additives	Con. (%)[b]	Sel. (%)[c]
1	BQ	8	99
2	DABCO	99	99
3	IPA	99	99
4	$AgNO_3$	12	99
5	KI	32	99

[a]Reaction: 7.4 mg of **1Tb**, 0.2 mmol benzyl thiol, 0.2 mmol TEA, DMF/MeCN (*V*/*V* = 4/1, 1mL), under visible light irradiation for 8 hours, O_2 atmosphere. [b,c]Conversion and selectivity were determined by GC. BQ, DABCO, IPA, $AgNO_3$ or KI (0.2 mmol) was added to quench superoxide radical, singlet oxygen, hydroxyl radical, electron and hole, respectively.

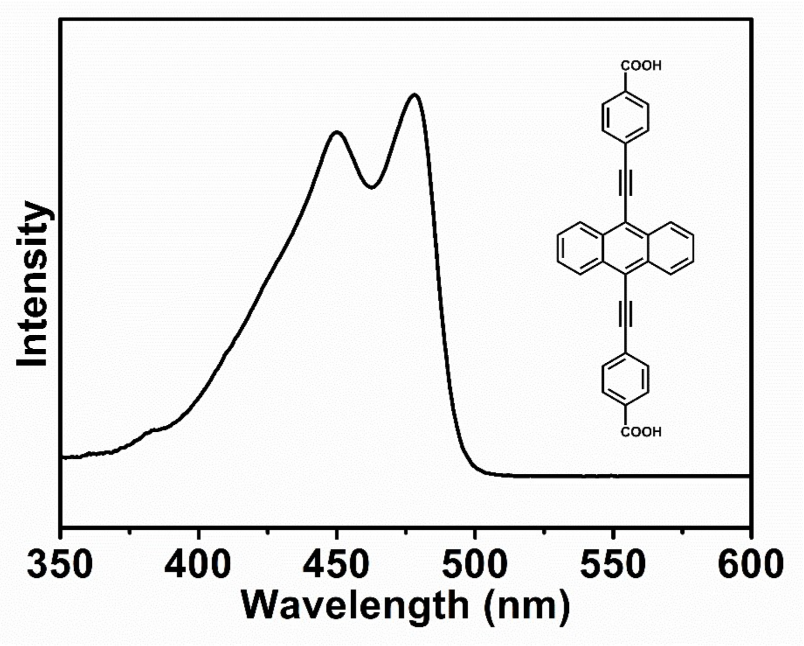

Fig. S1 UV-vis spectrum of ADBEB in DMF.

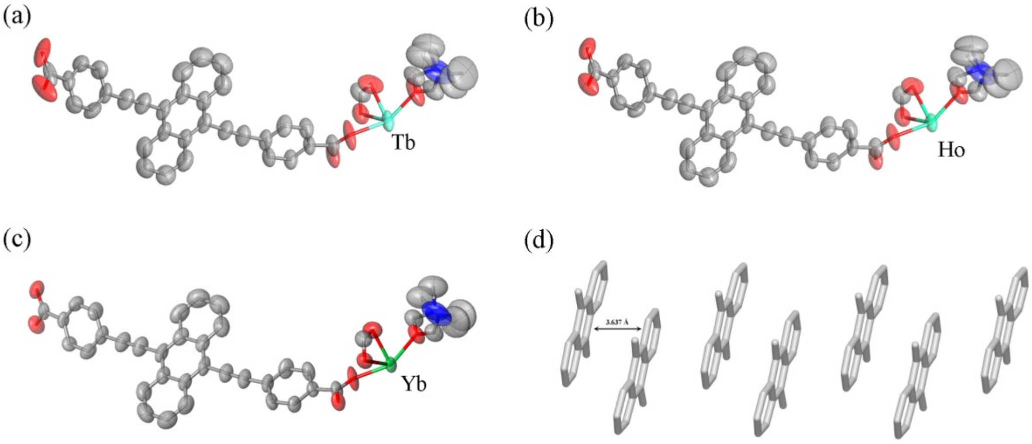

Fig. S2 (a)-(c) Asymmetric units of the synthesized CPs showing ADPs of the atoms. Gray, blue and red represent carbon, nitrogen and oxygen atoms, respectively. (d) Stacking between anthracene chromophores in adjacent ADBEB ligands.

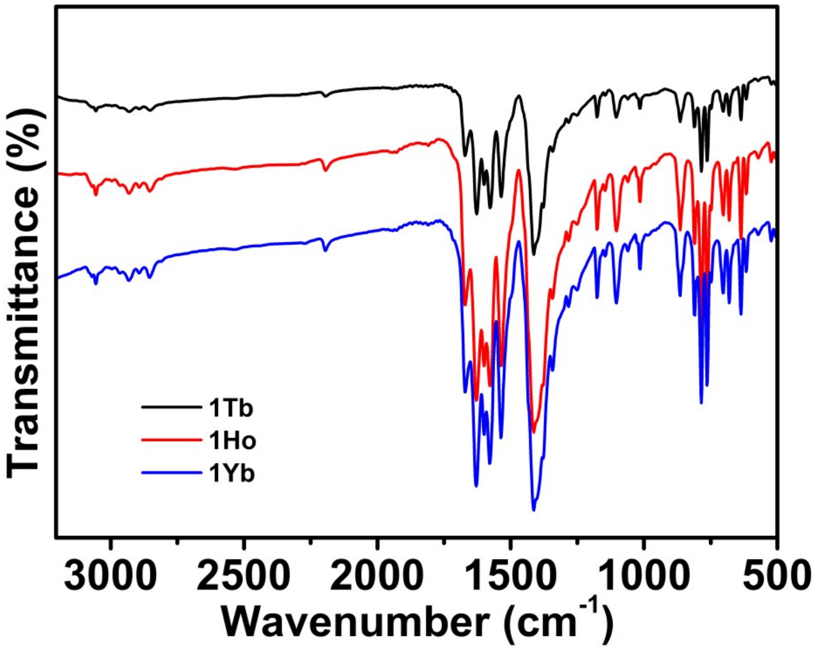

Fig. S3 FTIR spectra of Ln-CPs.

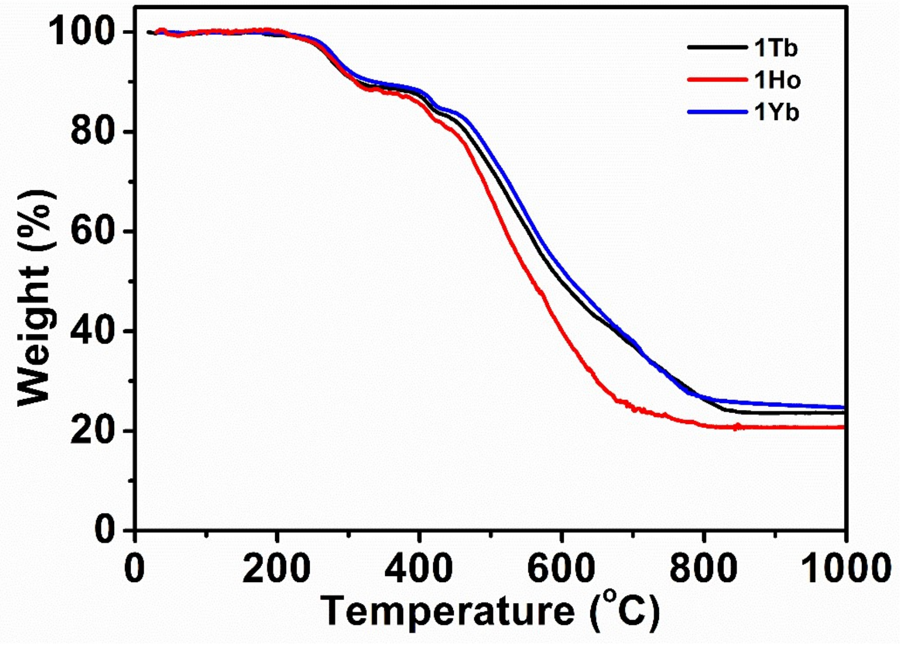

Fig. S4 TG curves of Ln-CPs.

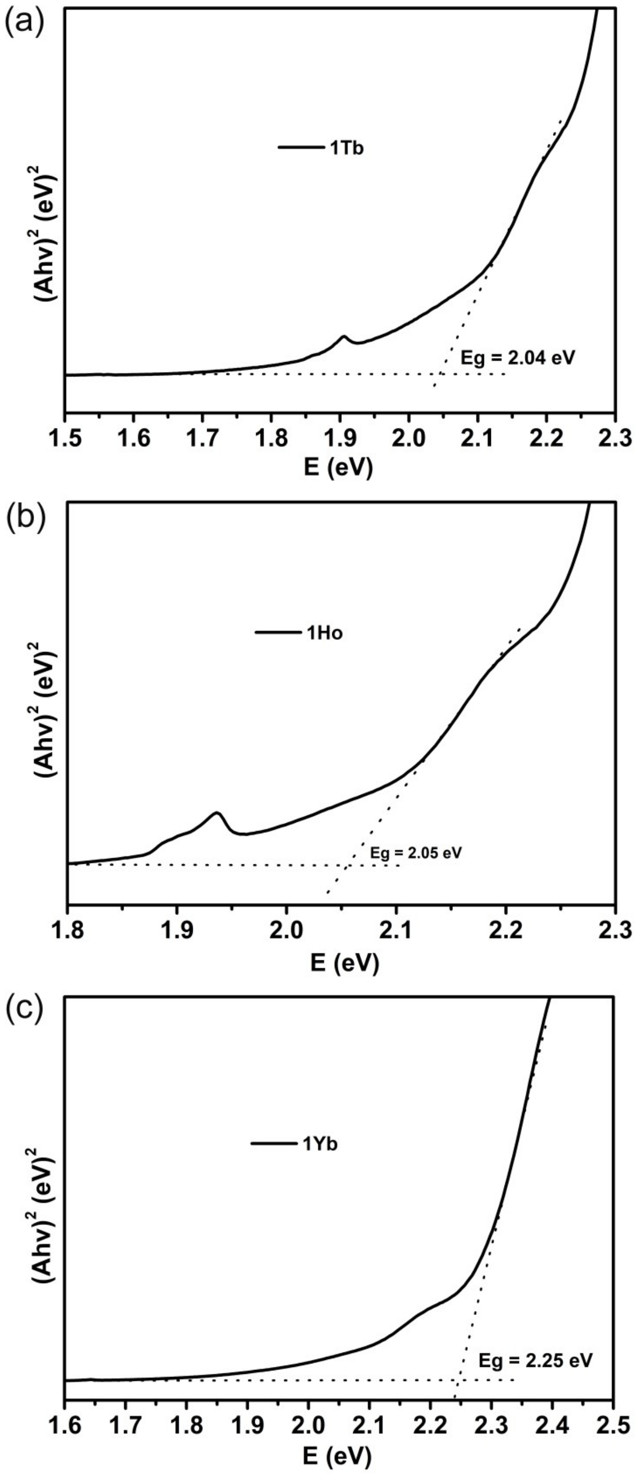

Fig. S5 Touc plots of Ln-CPs

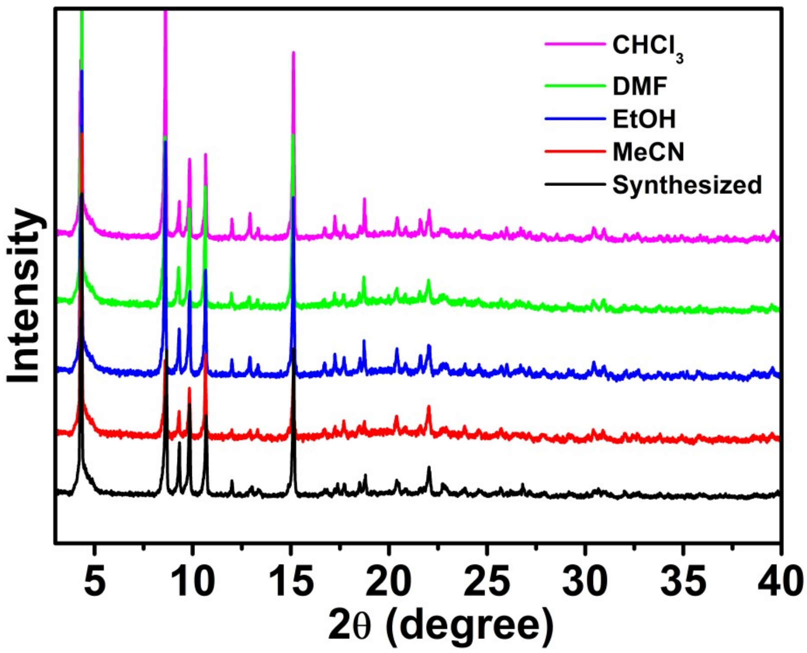

Fig. S6 PXRD patterns of **1Tb** in different organic solvents.

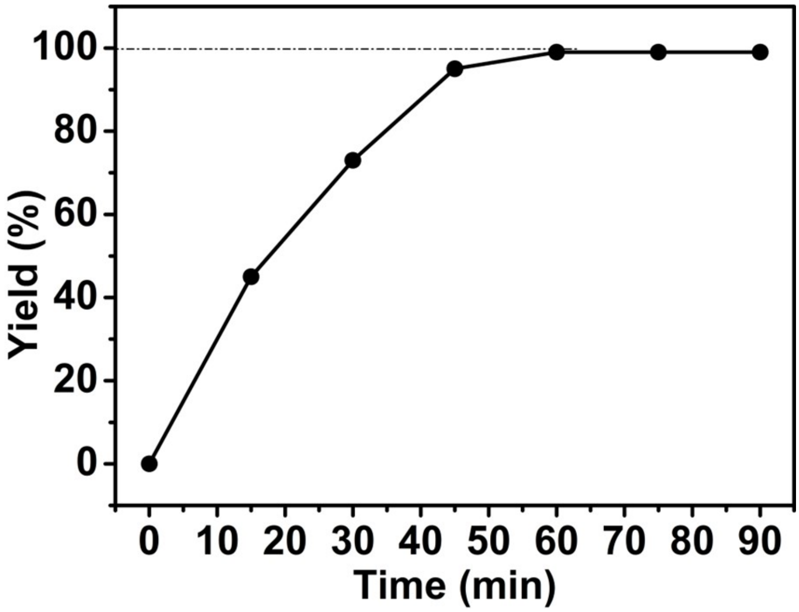

Fig. S7 Yield versus reaction time for the reaction of **1Tb**-mediated aerobic oxidation of benzylamine under visible light.

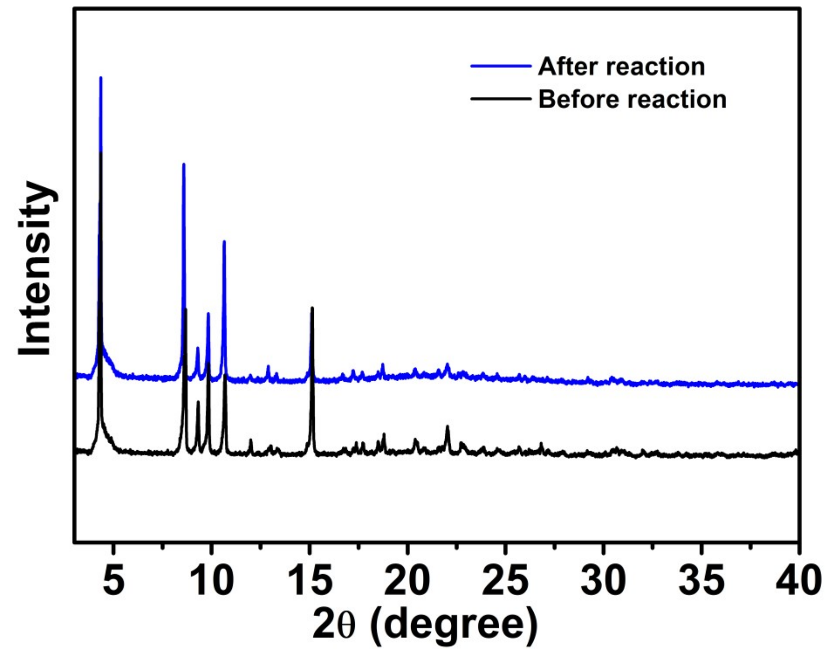

Fig. S8 PXRD patterns of **1Tb** before and after photocatalytic aerobic oxidation of benzylamine.

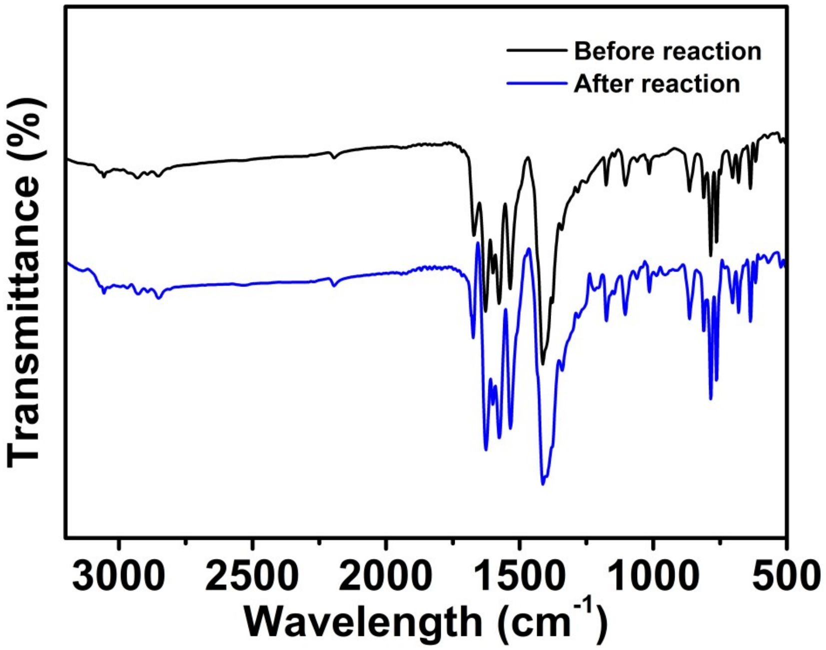

Fig. S9 The FTIR spectrum of **1Tb** before and after photocatalytic aerobic oxidation of benzylamine.

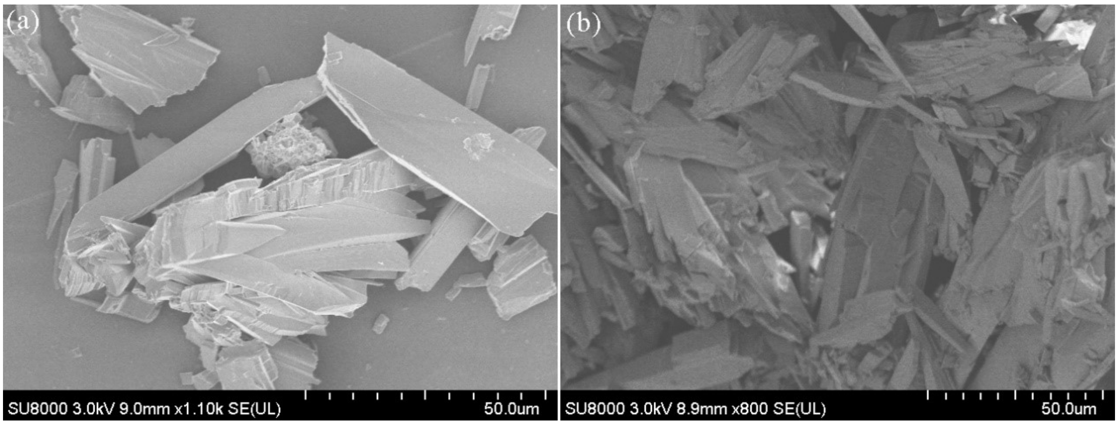

Fig. S10 SEM images of **1Tb** before and after photocatalytic aerobic oxidation of benzylamine.

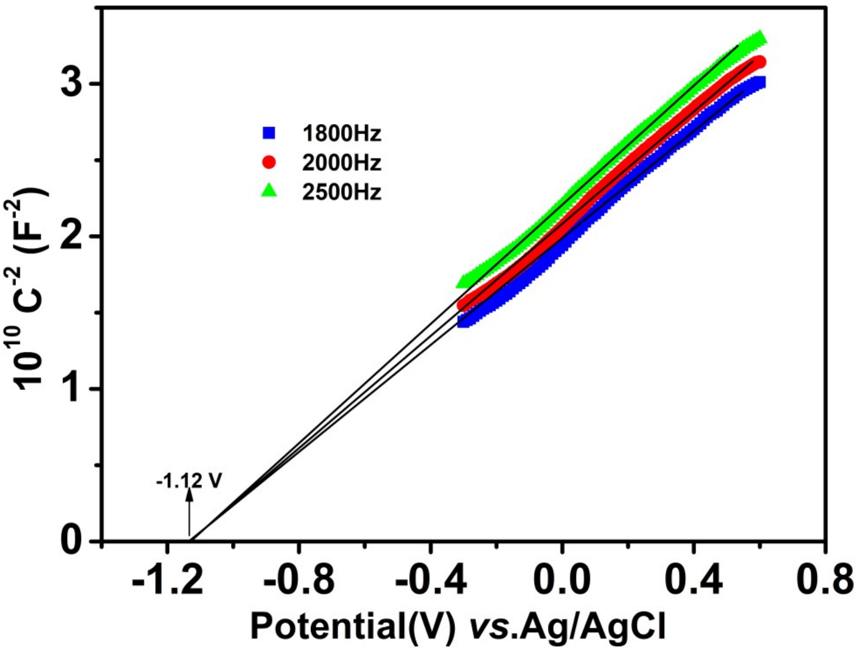

Fig. S11 Mott-Schottky plots of **1Tb** in 0.2 M Na_2SO_4.

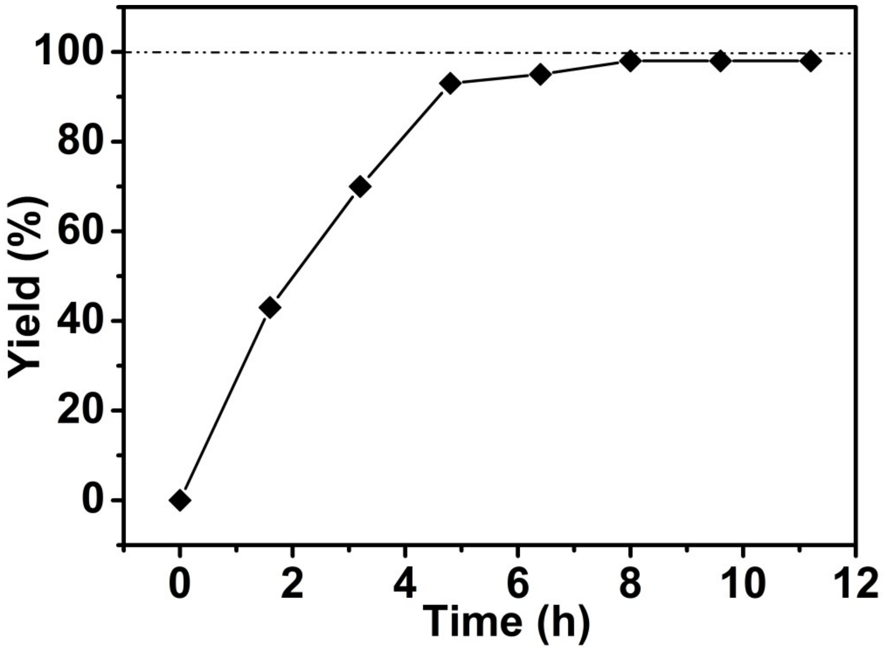

Fig. S12 Yield versus reaction time for the **1Tb**-mediated aerobic oxidation of thiol under visible light.

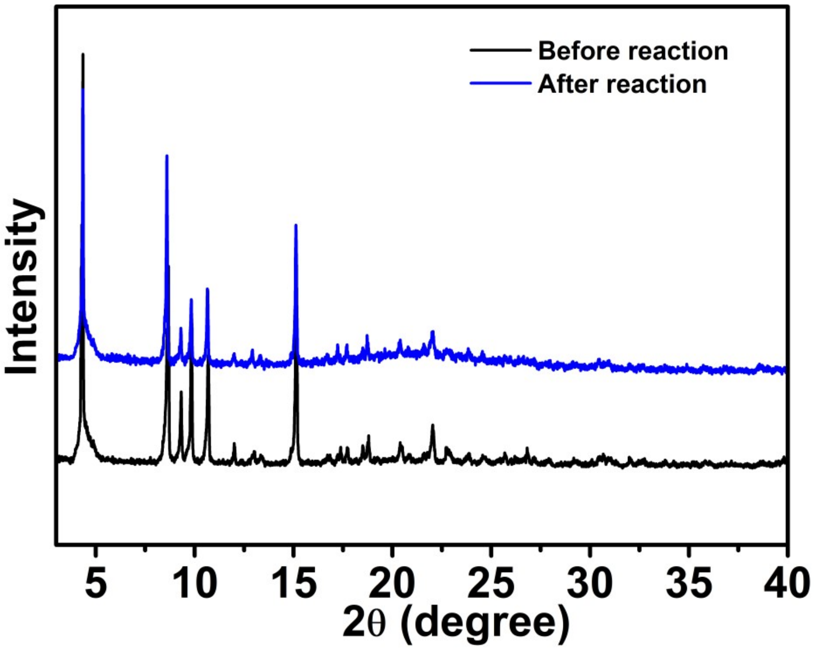

Fig. S13 PXRD patterns of **1Tb** before and after photocatalytic aerobic oxidation of thiol.

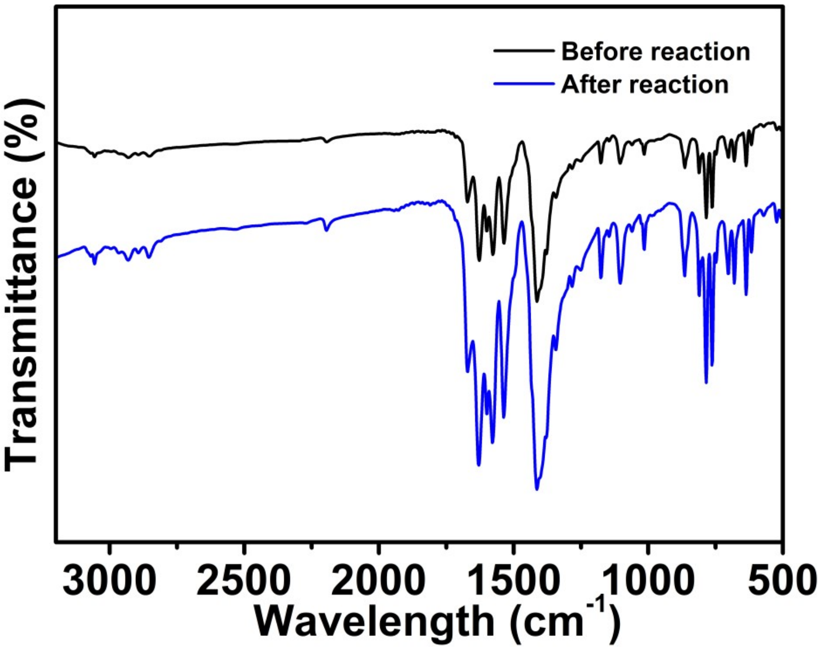

Fig. S14 FTIR spectra of **1Tb** before and after photocatalytic aerobic oxidation of thiol.

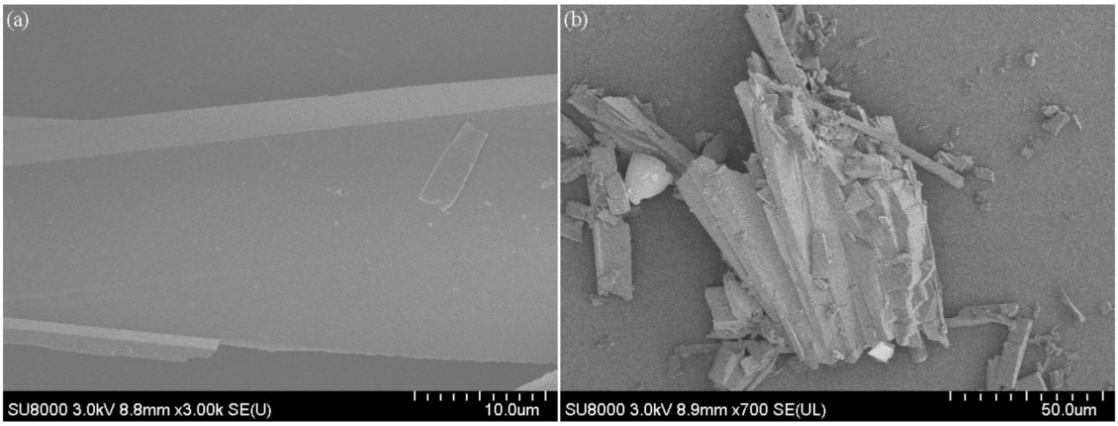

Fig. S15 SEM of **1Tb** before and after photocatalytic aerobic oxidation of thiol.

^{1}H-NMR spectrum data

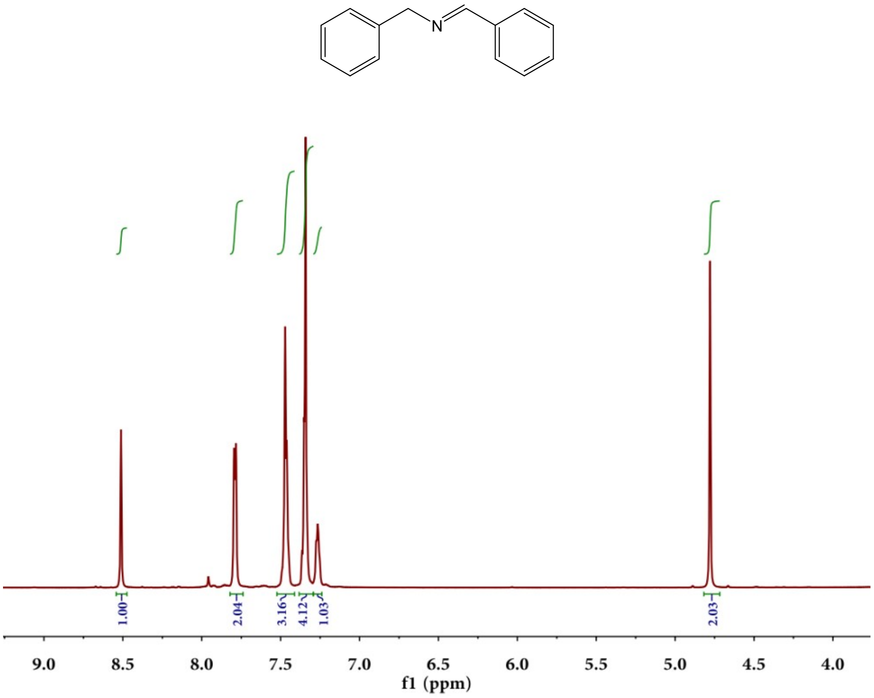

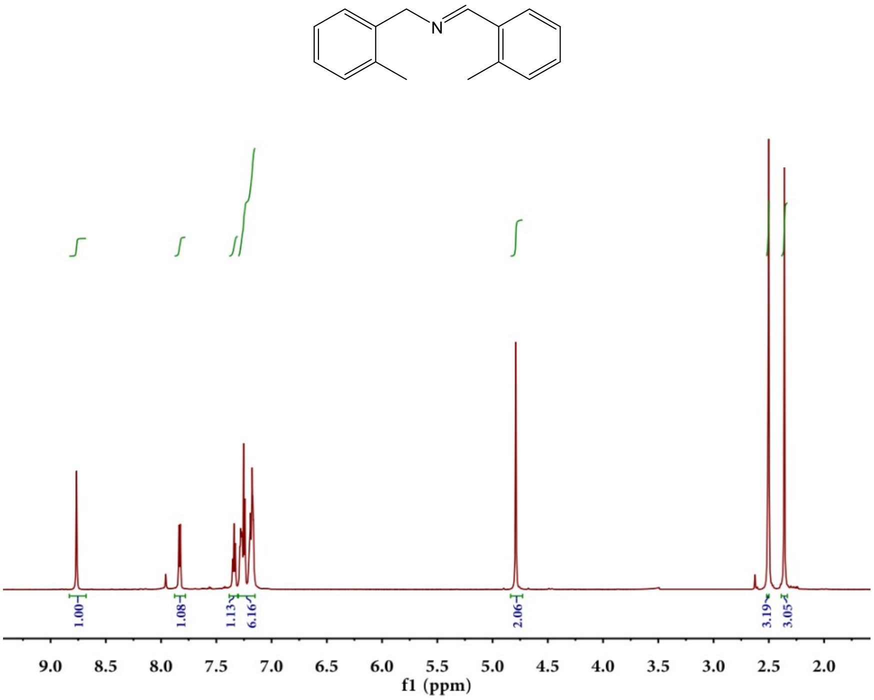

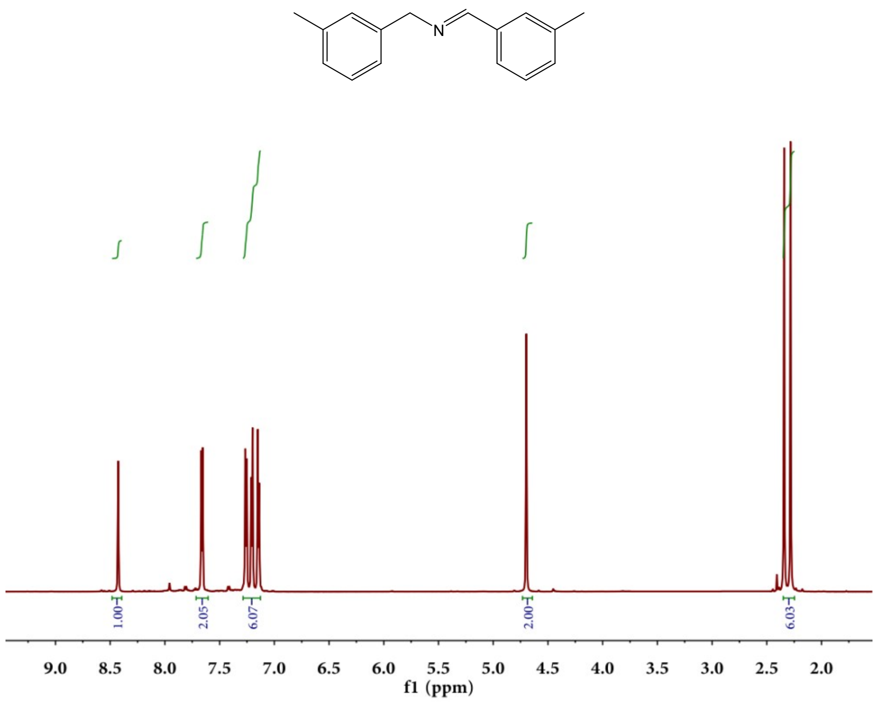
N
1.00
2.05
6.07
2.00
6.03
9.0 8.5 8.0 7.5 7.0 6.5 6.0 5.5 5.0 4.5 4.0 3.5 3.0 2.5 2.0
f1 (ppm)

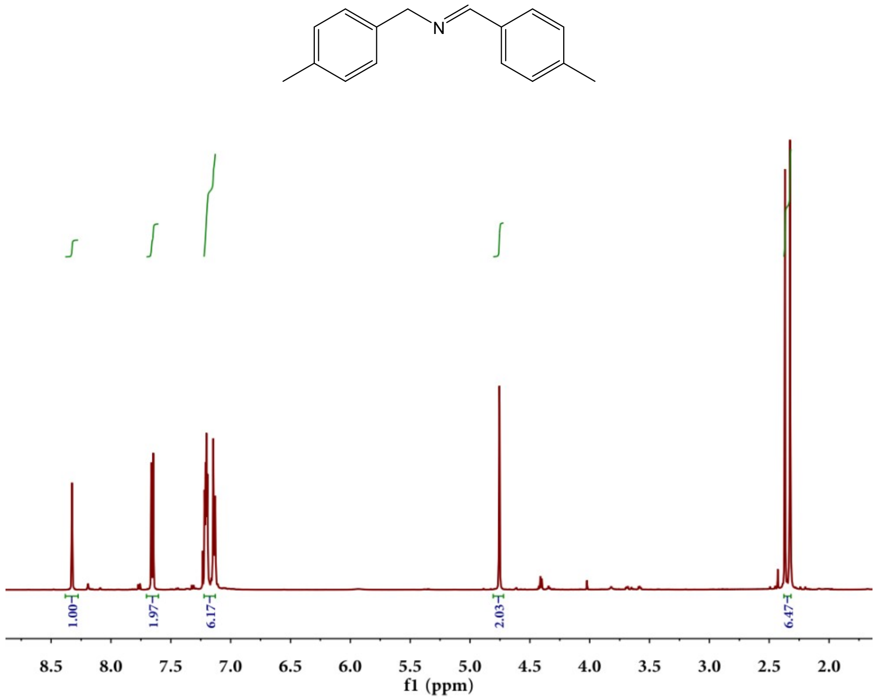
N
1.00
1.97
6.17
2.03
6.47
8.5 8.0 7.5 7.0 6.5 6.0 5.5 5.0 4.5 4.0 3.5 3.0 2.5 2.0
f1 (ppm)

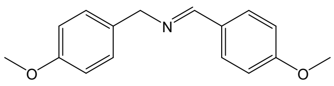
N
O
O

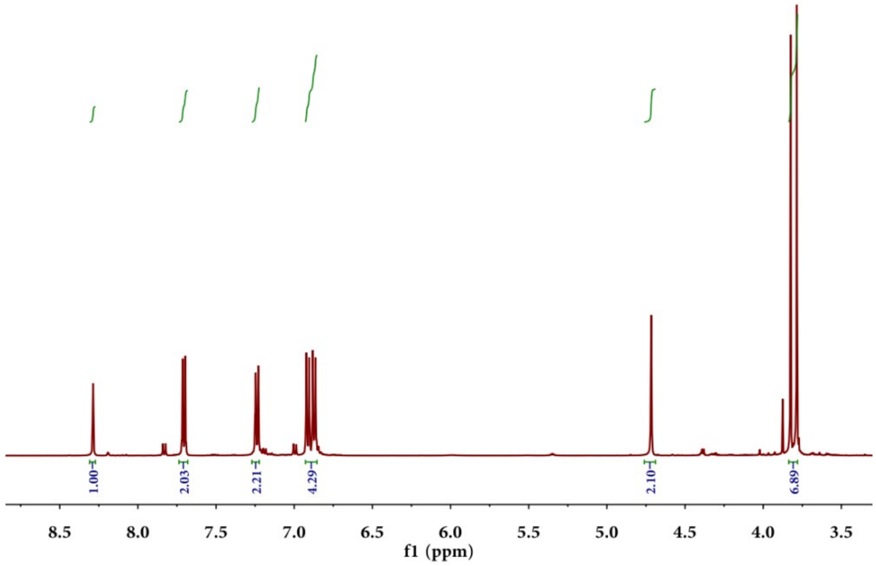
1.00
2.03
2.21
4.29
2.10
6.89
8.5
8.0
7.5
7.0
6.5
6.0
5.5
5.0
4.5
4.0
3.5
f1 (ppm)

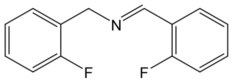
N
F
F

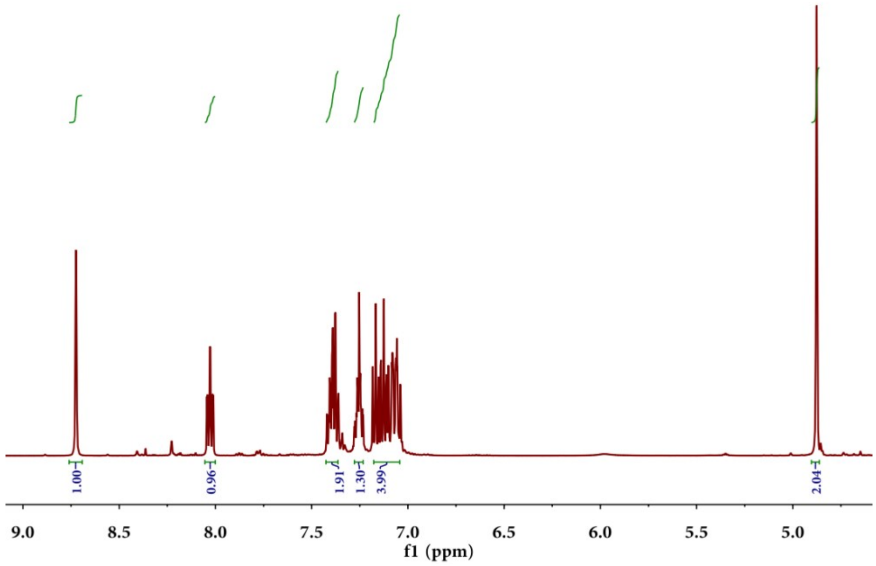
1.00
0.96
1.91
1.30
3.99
2.04
9.0
8.5
8.0
7.5
7.0
6.5
6.0
5.5
5.0
f1 (ppm)

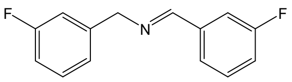
F
N
F

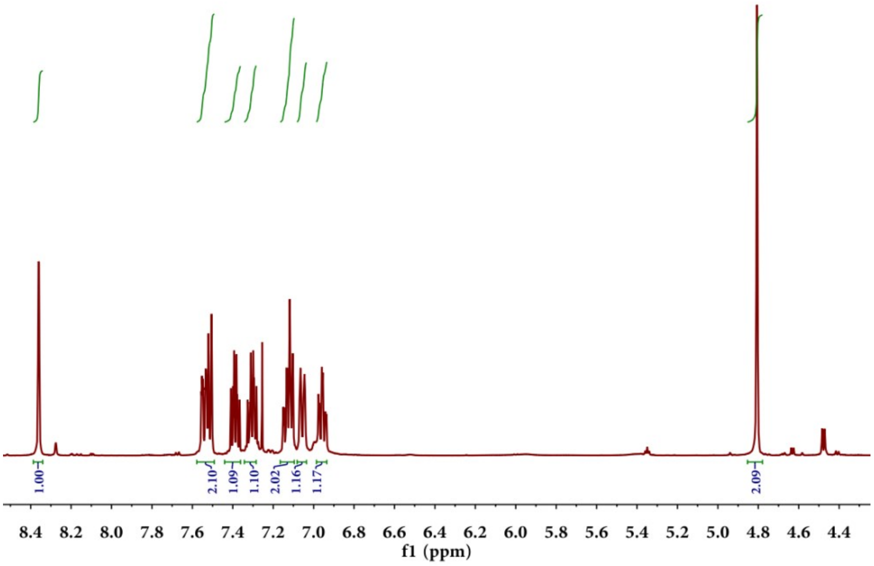
1.00
2.10
1.09
1.10
2.02
1.16
1.17
2.09
8.4 8.2 8.0 7.8 7.6 7.4 7.2 7.0 6.8 6.6 6.4 6.2 6.0 5.8 5.6 5.4 5.2 5.0 4.8 4.6 4.4
f1 (ppm)

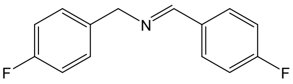
N
F
F

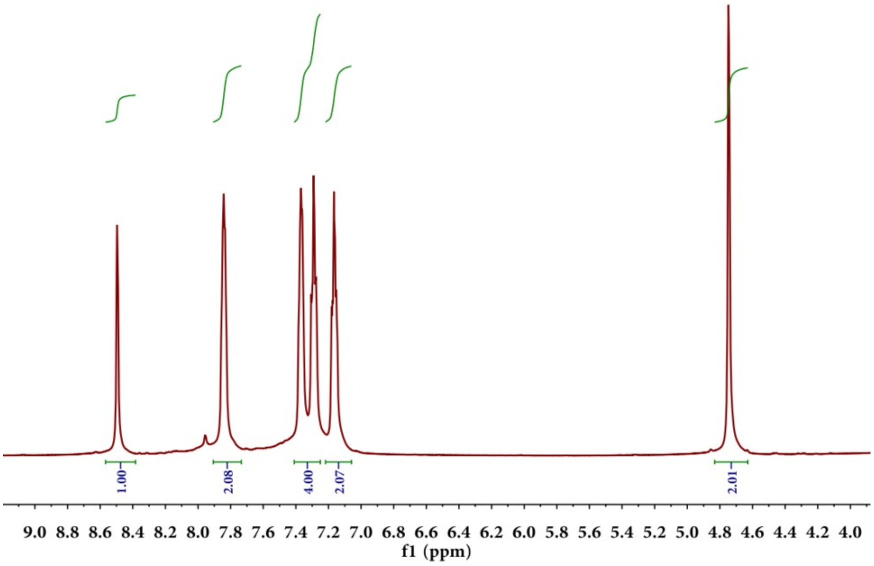
1.00
2.08
4.00
2.07
2.01
9.0 8.8 8.6 8.4 8.2 8.0 7.8 7.6 7.4 7.2 7.0 6.8 6.6 6.4 6.2 6.0 5.8 5.6 5.4 5.2 5.0 4.8 4.6 4.4 4.2 4.0
f1 (ppm)

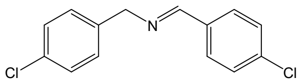
N
Cl
Cl

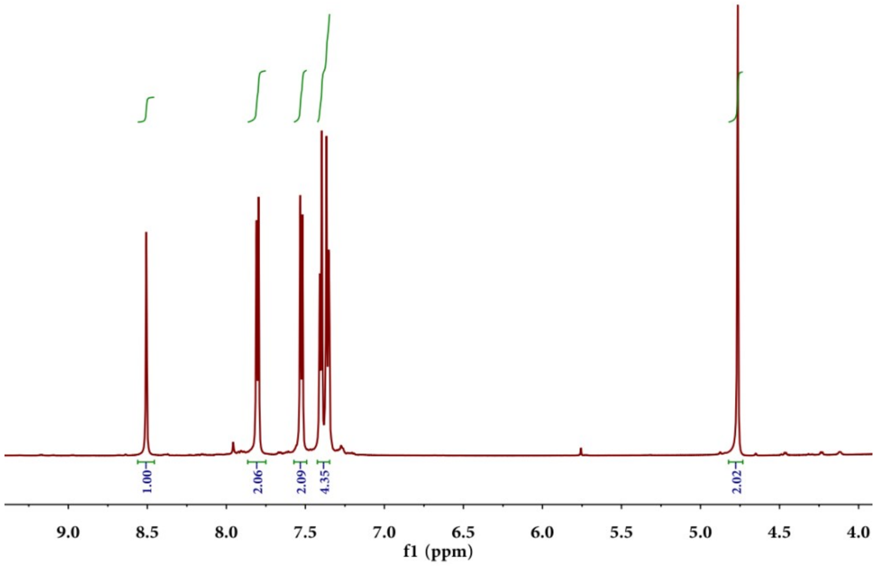
1.00
2.06
2.09
4.35
2.02
9.0
8.5
8.0
7.5
7.0
6.5
6.0
5.5
5.0
4.5
4.0
f1 (ppm)

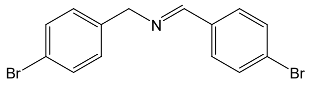
N
Br
Br

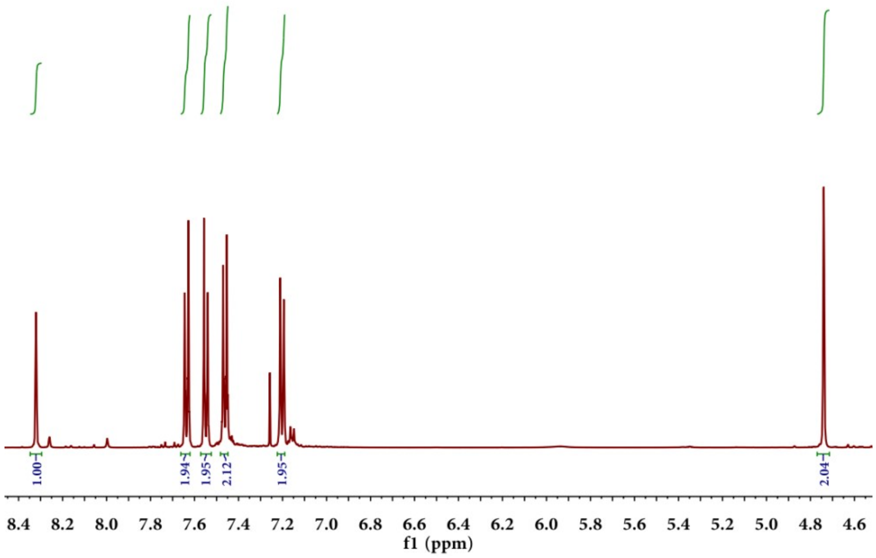
1.00
1.94
1.95
2.12
1.95
2.04
8.4
8.2
8.0
7.8
7.6
7.4
7.2
7.0
6.8
6.6
6.4
6.2
6.0
5.8
5.6
5.4
5.2
5.0
4.8
4.6
f1 (ppm)

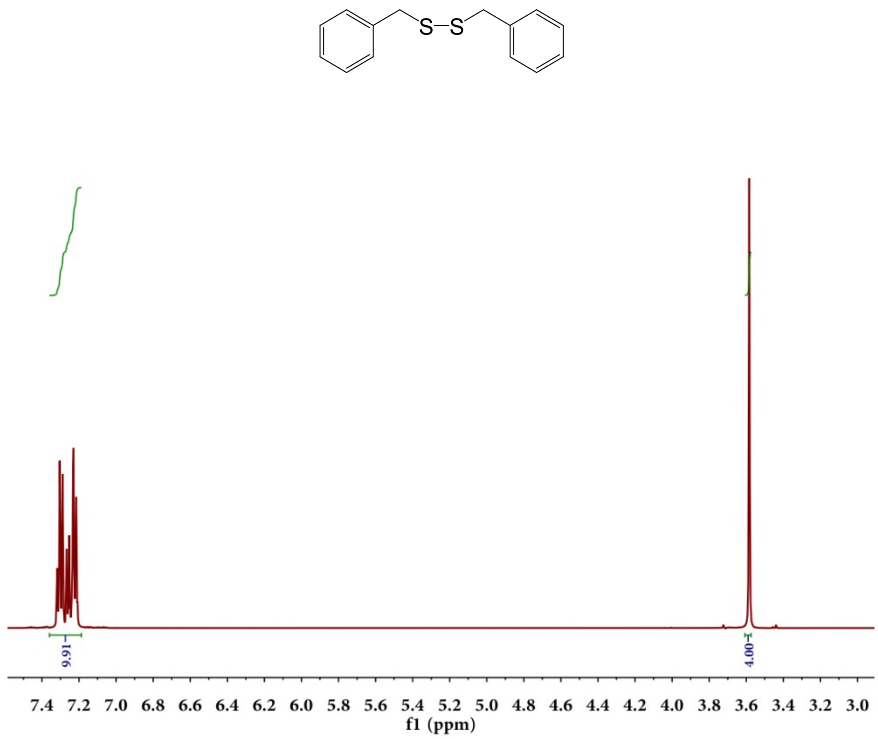
S
S
9.91
4.00
7.4 7.2 7.0 6.8 6.6 6.4 6.2 6.0 5.8 5.6 5.4 5.2 5.0 4.8 4.6 4.4 4.2 4.0 3.8 3.6 3.4 3.2 3.0
f1 (ppm)

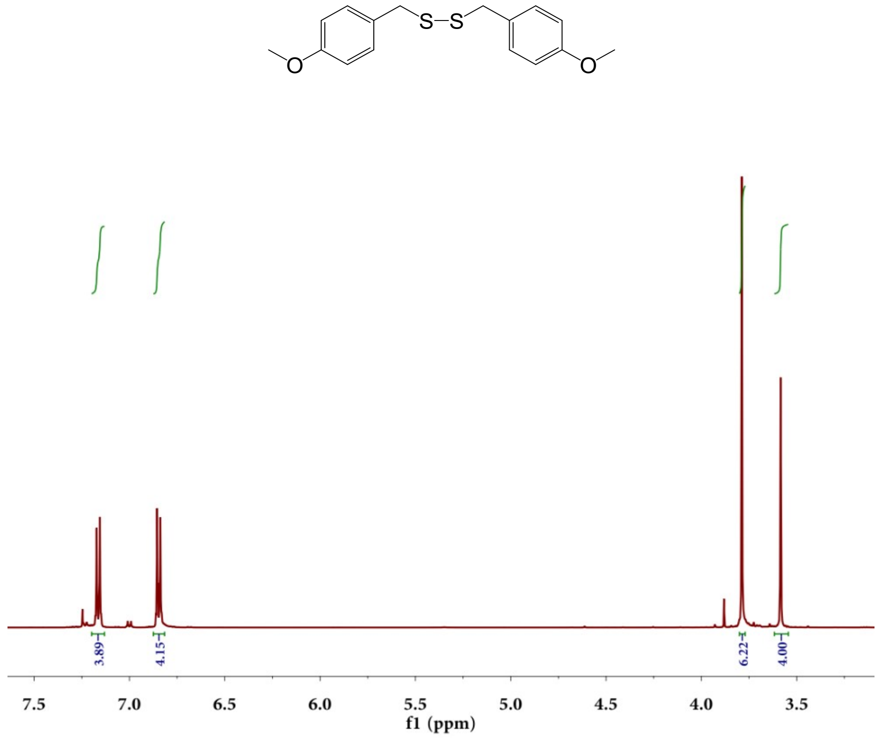
S
S
O
O
3.89
4.15
6.22
4.00
7.5 7.0 6.5 6.0 5.5 5.0 4.5 4.0 3.5
f1 (ppm)

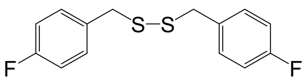

F
S
S
F

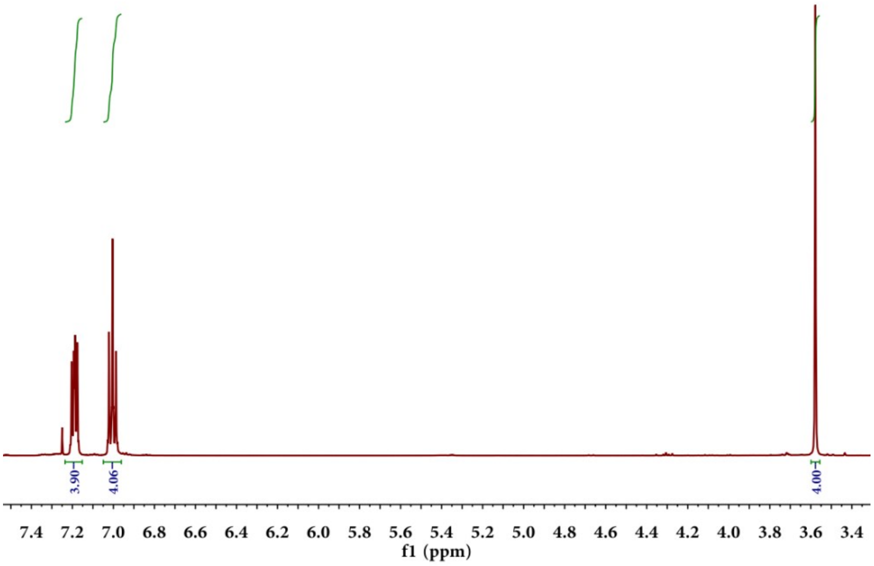

3.90
4.06
4.00
7.4 7.2 7.0 6.8 6.6 6.4 6.2 6.0 5.8 5.6 5.4 5.2 5.0 4.8 4.6 4.4 4.2 4.0 3.8 3.6 3.4
f1 (ppm)

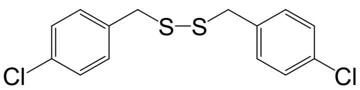

Cl
S
S
Cl

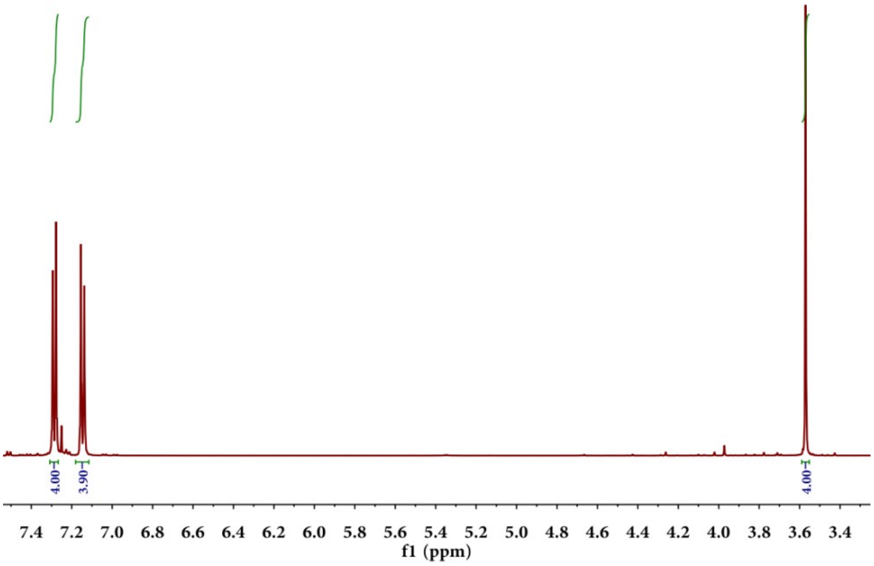

4.00
3.90
4.00
7.4 7.2 7.0 6.8 6.6 6.4 6.2 6.0 5.8 5.6 5.4 5.2 5.0 4.8 4.6 4.4 4.2 4.0 3.8 3.6 3.4
f1 (ppm)

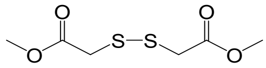
O
O
S
S
O
O

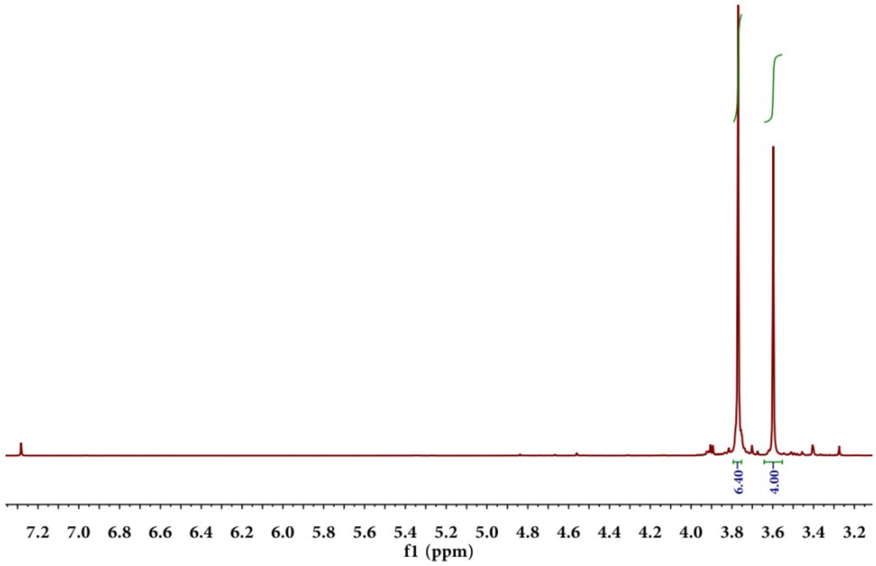
6.40
4.00
7.2
7.0
6.8
6.6
6.4
6.2
6.0
5.8
5.6
5.4
5.2
5.0
4.8
4.6
4.4
4.2
4.0
3.8
3.6
3.4
3.2
f1 (ppm)

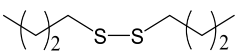
2
S
S
2

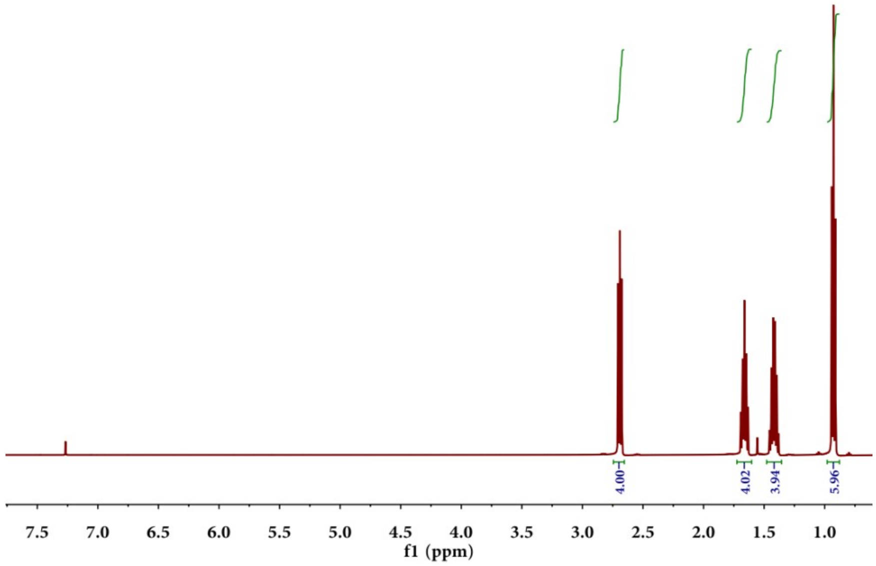
4.00
4.02
3.94
5.96
7.5
7.0
6.5
6.0
5.5
5.0
4.5
4.0
3.5
3.0
2.5
2.0
1.5
1.0
f1 (ppm)

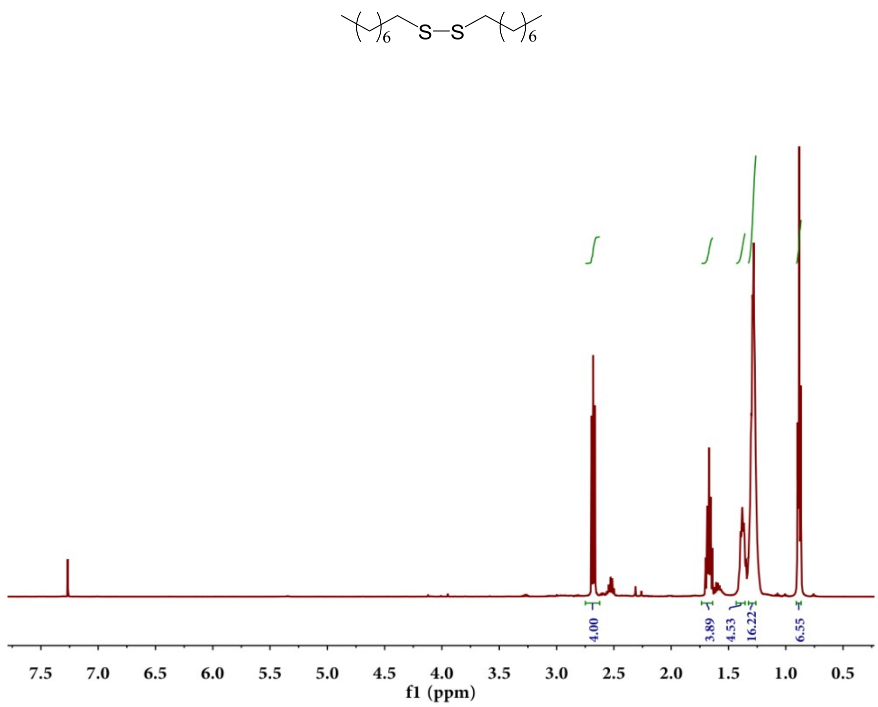
S
S
6
6
4.00
3.89
4.53
16.22
6.55
7.5
7.0
6.5
6.0
5.5
5.0
4.5
4.0
3.5
3.0
2.5
2.0
1.5
1.0
0.5
f1 (ppm)

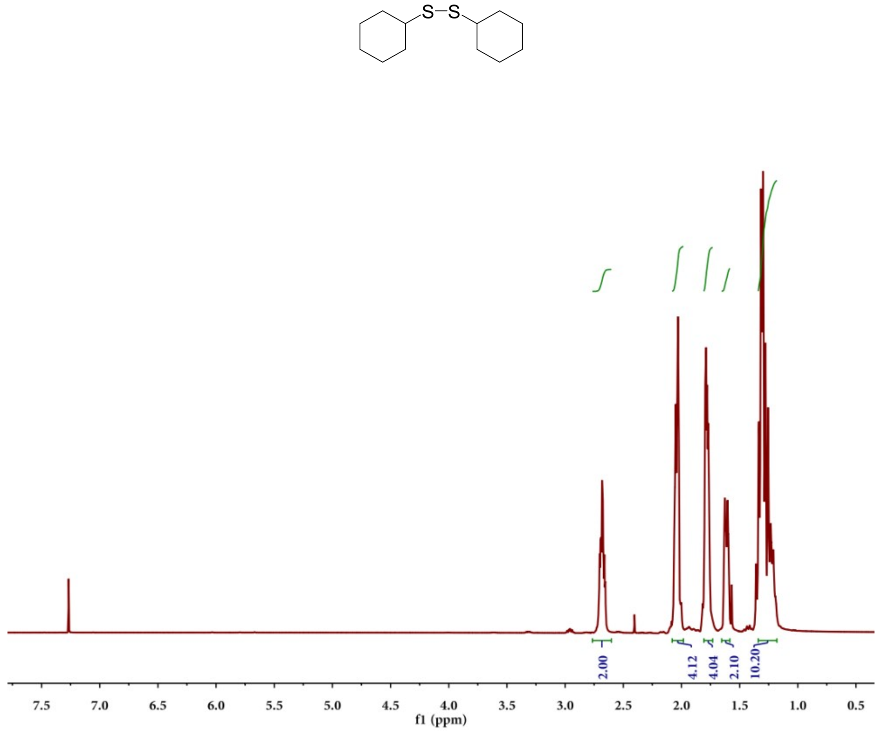
S
S
2.00
4.12
4.04
2.10
10.20
7.5
7.0
6.5
6.0
5.5
5.0
4.5
4.0
3.5
3.0
2.5
2.0
1.5
1.0
0.5
f1 (ppm)

References

1. D. Chen, H. Xing, C. Wang and Z. Su, *J. Mater. Chem. A,* 2016, **4**, 2657–2662.
2. F. Yu, Y-M. Zhang, Y-H. Guo, A-H. Li, G-X. Yua and B. Li, *CrystEngComm*., 2013, **15**, 8273–8279.
3. H.-Q. Xu, J. Hu, D. Wang, Z. Li, Q. Zhang, Y. Luo, S.-H. Yu and H.-L. Jiang, *J. Am. Chem. Soc.,* 2015, **137**, 13440−13443.
4. L. Krause, R. Herbst-Irmer and D. Stalke, *J. Appl. Cryst.,* 2015, **48**, 1907–1913.
5. G. M. Sheldrick, *Acta Cryst*., 2015, **C71**, 3–8.
6. L. M. Aguirre-Díaz, N. Snejko, M. Iglesias, F. Sánchez, E. Gutiérrez-Puebla and M. A. Monge, *Inorg. Chem*., 2018, **57**, 6883–6892.
7. R. Liu, S. Meng, Y. Ma, L. Niu, S. He, X. Xu, B. Su, D. Lu, Z. Yang and Z. Lei, *Catal. Commun*., 2019, **124**, 108–112.
8. D. Sun, L. Ye and Z. Li, *Appl. Catal. B: Environ*., 2015, **164**, 428-432.
9. J. Shi, J. Zhang, T. Liang, D. Tan, X. Tan, Q. Wan, X. Cheng, B. Zhang, B. Han, L. Liu, F. Zhang and G. Chen, *ACS Appl. Mater. Interfaces,* 2019, **11**, 30953−30958.
10. Y. Sha, J. Zhang, D. Tan, F. Zhang, X. Cheng, X. Tan, B. Zhang, B. Han, L. Zheng and J. Zhang, *Chem. Commun*., 2020, **56**, 10754−10757.
11. H. Wei, Z. Guo, X. Liang, P. Chen, H. Liu and H. Xing, *ACS Appl. Mater. Interfaces,* 2019, **11**, 3016–3023.
12. L. Zeng, T. Liu, C. He, D. Shi, F. Zhang and C. Duan, *J. Am. Chem. Soc*., 2016, **138**, 3958−3961.
13. C. Xu, H. Liu, D. Li, J.-H. Su and H.-L. Jiang, *Chem. Sci*., 2018, **9**, 3152–3158.